Proceedings of the International Symposium on Engineering Lessons Learned from
the 2011 Great East Japan Earthquake, March 1-4, 2012, Tokyo, Japan

TSUNAMI SIMULATION FOR THE 2011 GREAT TOHOKU EARTHQUAKE USING SEISMIC INVERSION SOURCE MODEL AND FULLY NONLINEAR TSUNAMI MODEL

Anatoly PETUKHIN[1], Kunikazu YOSHIDA[2], Ken MIYAKOSHI[3] and Kojiro IRIKURA[4]

[1] Senior researcher, earthquake engineering group, Geo-Research Institute, Osaka, Japan, anatolyp@geor.or.jp
[2] Senior researcher, earthquake engineering group, Geo-Research Institute, Osaka, Japan, yoshida@geor.or.jp
[3] Group leader, earthquake engineering group, Geo-Research Institute, Osaka, Japan, ken@geor.or.jp
[4] Adjunct Professor, Aichi Institute of Technology, Professor Emeritus, Kyoto University, Japan, irikura@geor.or.jp

ABSTRACT: The question we addressing here is the possibility of evenly good simulation of observed ground motions and tsunami using the same source model. By comparing simulated and observed tsunami waves we test source inversion and characterization technique for M9 class event on example of the 2011 Tohoku earthquake. Simulation results fit observed tsunami waveforms in the off-shore area and reproduce inundation data in most of target region.

Key Words: Great East Japan earthquake, source characterization, nonlinear tsunami simulation

INTRODUCTION

On March 11, 2001, M9.0 earthquake has occurred east off the Pacific coast of Tohoku, as a result of thrust faulting on the interface of plate boundary between the Pacific and North American plates. This earthquake generated tsunami of 30-40m high and strong ground motions up to 1000gal and more. This is one of the best geophysically-recorded great earthquakes and due to this numerous source models were generated using teleseismic, GPS, strong ground motion and tsunami data (e.g. Hayes 2011; Ide et al. 2011; Ito et al. 2011; Lay et al. 2011; Satake et al. 2011).

The question we addressing here is the possibility of evenly good simulation of observed ground motions and tsunami using the same source model. In this case we could use source modeling techniques, which were developed for the strong-ground motion prediction (Irikura and Miyake 2010), for the modeling of tsunami sources and prediction of possible tsunamis. A basement of the seismic

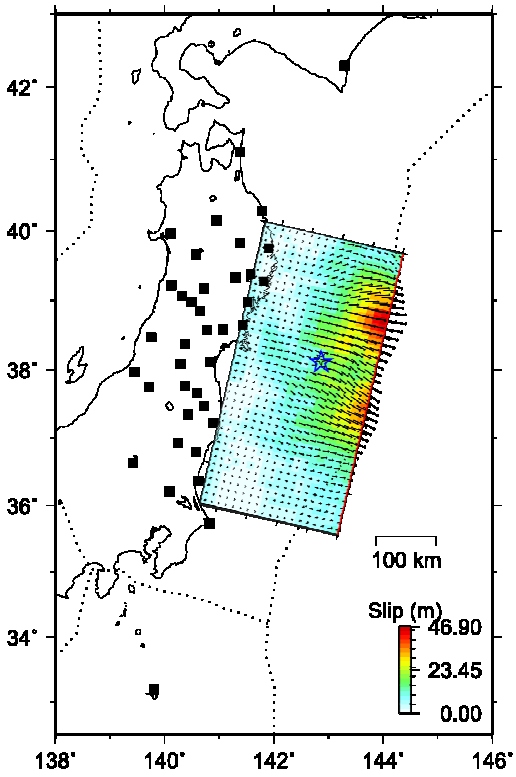

Fig. 1 Final slip distribution of the source model (Yosida et al. 2011). The star and squares indicate the rupture starting point and the strong-motion stations that are used for the inversion. Dotted line shows plate boundaries (Bird, 2003)

source modeling is scaling relations between source parameters, e.g. fault area size, asperity area size, slip value from one side, and seismic moment from another side (Somerville at al. 1999; Murotani et al., 2008). These scaling relations are estimated by generalization of the seismic source inversion results. As the first step, by comparing simulated and observed tsunami waves we will test source inversion technique on example of the 2011 Tohoku earthquake.

SOURCE MODEL

Here we used rupture process of the 2011 Tohoku earthquake inverted by the multi-time window linear waveform inversion method using the long-period (20-200s) strong-ground motion data (Yoshida et al. 2011). Effects of complicated 3D velocity structure in subduction zone (effects of accretion prism and subducting plate) are negligible in this period range. For this reason accurate and computationally effective discrete wavenumber method of Bouchon (1981) combined with 1D propagator matrix algorithm of Kennet and Kerry (1979) can be used for calculation of the Green's functions. From another side, signal-to-noise ratio of 20-200s long-period ground motions is large enough for the *Mw*9.0 earthquake. Velocity records at very hard bedrock sites of the F-net, KiK-net and Hokkaido University seismic networks were used for inversion. A single planar fault model of 475 km in strike and 240 km in dip is assumed. The rupture velocity inferred to be slower than 2.5 km/s at early stage of the rupture process. The seismic moment of this earthquake was estimated to be $4.3e10^{22}$ Nm (*Mw* = 9.0).

The inverted slip distribution shows a large elongated asperity (large slip area) with a maximum slip of 47 m which is located on the shallower part of the fault plane, slightly north of epicenter (Fig. 1). This is consistent with other source models (e.g. Ide et al. 2011; Lay et al. 2011). Area of the moment rate large amplitudes, which is responsible for generation of short period ground motions, is

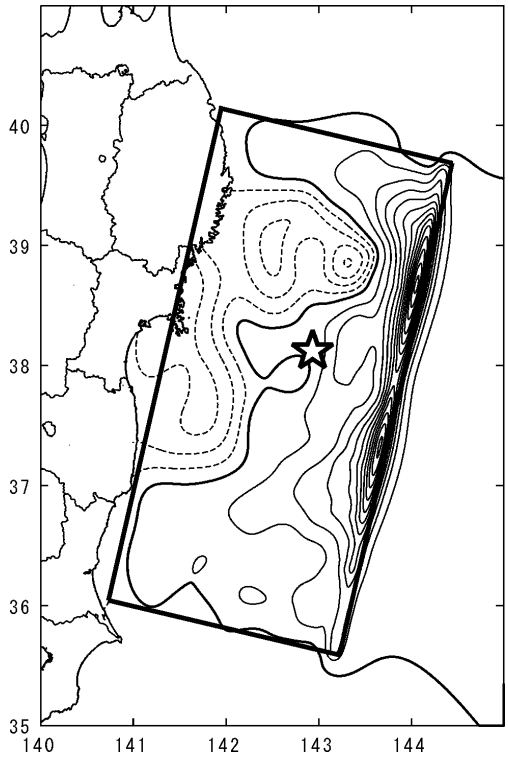

Fig. 2 Distribution of the sea surface elevation due to the source slip. Solid contours (1m interval) indicate uplift, dashed contours (0.5m interval) – subsidence, thick contour – zero elevation, points – source model subfaults, star – epicenter location

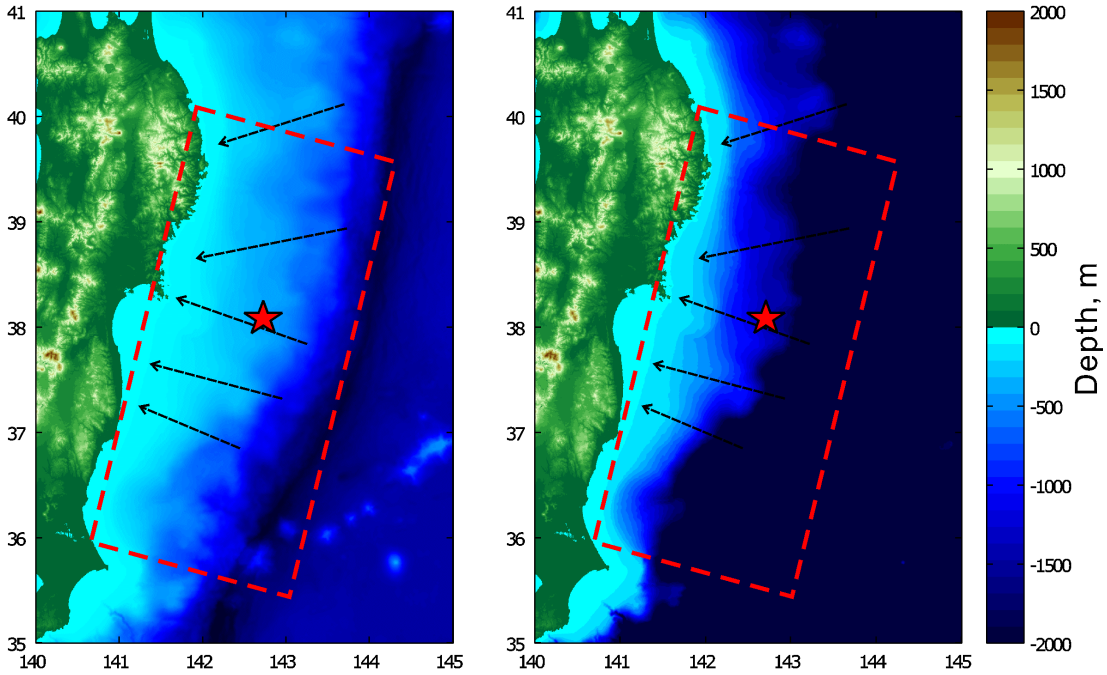

Fig. 3 Bathimetry map of the target area. Arrows indicate seafloor ridges, which are potential waveguides of tsunami waves. Red line and star mark indicates source plane and earthquake epicenter. Bathymetry map on the right plot is scaled to 2000m for clarity

shifted to deeper part of the source and have tendency to scatter in a few strong motion generation areas. This is consistent with the empirical Green's function simulation results of Kurahashi and Irikura (2011). The rupture process is divided into three stages: first stage with moderate slip; second stage with large and long-duration slip in the shallow part of the fault; and third stage with relatively small and short-duration slip in the southern part of the fault. Rupture velocity is around 3–4 km/s in the first and third stages, while rupture progression suspended for a while before the rupture of the asperity.

TSUNAMI SIMULATION

Numerical simulations of tsunami require three components: (1) source model, reflecting fault location and slip distribution; (2) ocean bathymetry and coastal topography, and (3) tsunami propagation and inundation model.

Seafloor displacement modeled as a sum effect of all seismic subsources of the source model, which are classical dislocation point sources, combining slip motions occurring on the oblique fault plane embedded into semi-infinite elastic medium (Okada, 1985). Shear modulus equal 4.0×10^{10} kg/ms^2 is assumed. Sea surface elevation (Fig. 2) is then calculated using curve fitting technique of Watts et al. (2003). We used time dependent slip rate functions estimated by the multi-time window source inversion on each subfault. We also consider time delay of subsources due to rupture propagation. Although rupture velocity (~2000 m/s) is much higher than tsunami wave velocity (~500 m/s for deep water around trench), weak effect of rupture propagation is possible.

Model of ocean bathymetry and coastal topography is combined from the 500m gridded bathymetric data set J-EGG500 of the Japan Oceanographic Data Center (JDOC) and 250m gridded inland topography of the Digital Elevation Model from the Geospatial Information Authority of Japan (GSI). Bathymetry map is shown in Fig. 3. 500m grid gives enough resolution for tsunami propagation and inundation in off-shore area and in simple coast-line environment of Sendai plain and Fukushima prefecture in the southern part of the source region. However, in the northern part of source region, the Ria environment on the Sanriku coast is composed from numerous small size bays, many of them have only 1-3km size, which are just one-to-few grids of bathymetry model. Large simulation errors of inundation and run-up are possible here. Another source of the tsunami wave amplification is the propagation of wave along/above a submarine ridge. Wave velocity become smaller just above the ridge and higher in neighboring valleys. This results in the geometrical focusing effect increasing amplitude of tsunami wave, even in a flat coastal environment. In Fig. 3 potentially dangerous ridges are shown by arrows.

For tsunami propagation and inundation we use a Boussinesq water wave model developed by Wei and Kirby (1995) (program FUNWAVE). The model is fully nonlinear and dispersive, retaining information to all orders in nonlinearity a/h (where a - wave amplitude, and h - water depth). Program includes bottom dissipation and wave breaking, without which the wave would artificially amplify at the coast, and allows simulation of the land inundation through a moving shoreline algorithm, which has been fully validated for short-wave shoaling, breaking and run-up. Method has been calibrated to provide a stable model for tsunami run-up, and has been successfully used to simulate various regional earthquake tsunamis, including devastating 2004 Indian Ocean tsunami (e.g. Ioualalen et al., 2006). Simulation area of the 2011 Tohoku tsunami is limited to 140°-145°E and 35°-41°N, for simulation we used 500 m finite difference grid and 0.5 sec time step, number of steps is 11000.

TSUNAMI SIMULATION RESULTS

Results of tsunami simulation are compared with the off-shore gauge waveform data of the Nationwide Ocean Wave Information network for Ports and HArbourS (NOWPHAS, http://nowphas.mlit.go.jp/) and with on shore inundation data of the Tohoku Earthquake Tsunami

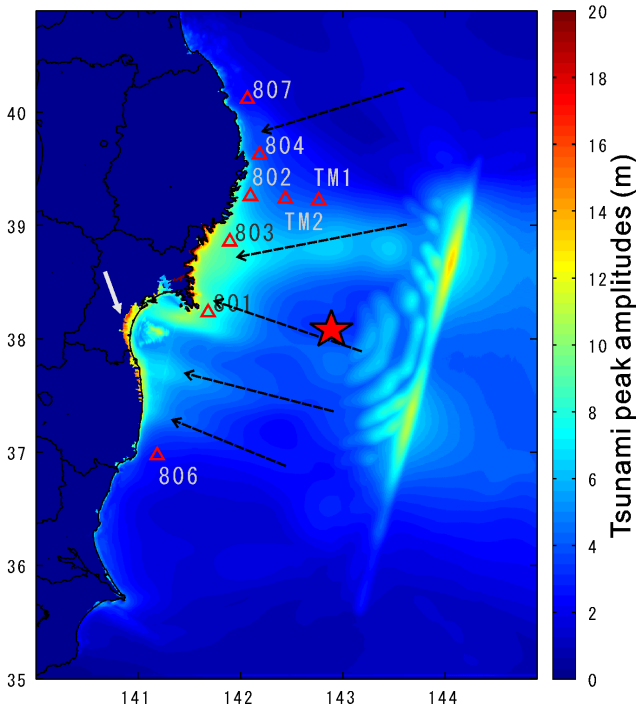

Fig. 4 Distribution of maximum amplitudes of propagated tsunami waves. Location of the offshore gauges (triangles) and waveguide ridges from Fig. 3 (dashed arrows) are shown for reference. White arrow points large run-up area in the Sendai plain

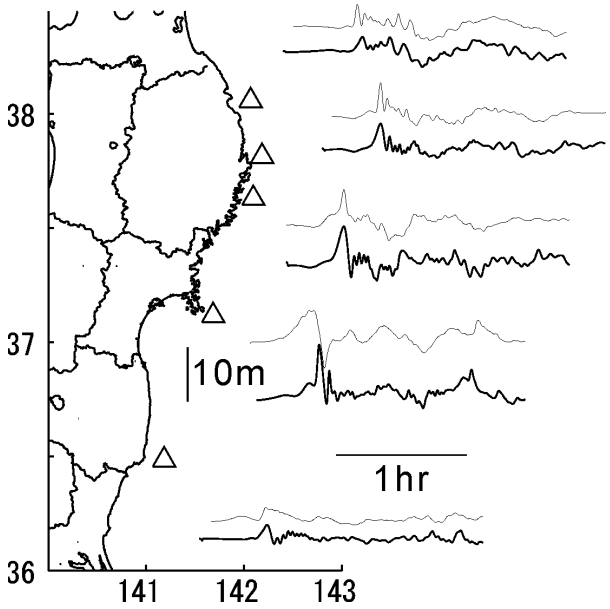

Fig. 5 Comparison of observed (upper) and simulated (lower) tsunami waveforms

Survey Group (release 20110601, http://www.coastal.jp/ttjt/). Many coastal tide gauges on the Tohoku coast were broken by the first tsunami wave. Two offshore floating GPS wave gauges number 804 and 802 at a 200m depth (see Fig. 4) and two cable pressure-gauges (TM-1 at 1600 m and TM-2 at 1000 m depth) are recorded unusual two-stage tsunamis (Fig. 5). The water level gradually increased up to 2 m during the first 10 minutes, and then impulsive tsunami wave having higher amplitude and shorter period was observed. At southern GPS gauge number 806, similar two pulses were recorded, although

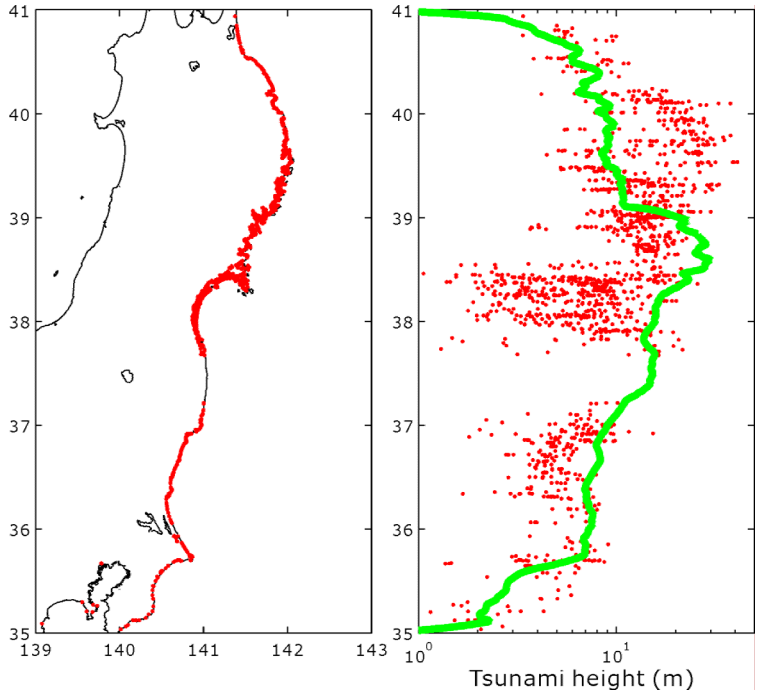

Fig. 6 Right: Comparison of observed inundation heights (dots) and simulated peak values (line) for the inverted source model of Yoshida et al. (2011). Left: Location of observation points

their periods were similar.

Simulation results fit observed tsunami waves in the off-shore area (Fig. 5), both direct wave and later phases, which we interpret as the reflected waves, and reproduce inundation data on the coast of the Sendai plain and in Fukushima (Fig. 6). Some variations of the inundation heights are possible both due to effect of waveguides (e.g. Central Fukushima area) and effect of coastal bathymetry (e.g. Northern Miyagi area). On the Sanriku coast, north of epicenter, simulated amplitudes are smaller than observed ones. Possible reason of the underestimated simulated amplitudes is a small resolution of used bathymetry data for this area, mentioned above. Simulated waveforms in general reproduce two-stage feature of the observed waveforms. We suppose that 1st stage is a result of tsunami generation in a wide subsidence area just north of epicenter, while 2nd stage is result of high uplift of the ocean surface on the edge of seismic source near the trench, see Fig. 2. This is supported by back projection analysis of tsunami arrival times of Hayashi et al. (2011), which show that primary crests of tsunami waves are generated in area centered at point 143.9E/38.5N.

TSUNAMI SIMULATION USING CHARACTERIZED SOURCE MODEL

For prediction of future tsunamis we could try to use source modeling techniques, which were developed for the strong-ground motion prediction (Irikura and Miyake 2010). A basement of the seismic source modeling is scaling relations between the characterized source parameters and seismic moment, which are result of generalization of the seismic source inversion results. Here we test source characterization technique for M9 class event on example of the 2011 Tohoku earthquake.

Fig. 7 shows result of characterization of the slip distribution from Fig. 1 using trimming technique of Somerville et al. (1999). Bold line indicates asperity. Parameters of the characterized source are shown in Table 1. On Fig. 8 these parameters are compared with the average relationships for subduction zone earthquakes of Murotani et al. (2008); good agreement is found.

At the next step we simulated tsunami using 500m grid similarly to the first case above. It is natural that pulse width becomes wider in case of characterized source model. For this reason waveform agreement become worth in the northern part (gauges 807, 804 and 802), but much better in

the southern part (gauges 803, 801 and 806). Contrary, maximum inundation heights distribution didn't change very much (compare Fig. 9 and Fig. 6). Maximum difference is around 40%, which is natural payment to the uncertainty of the source model. We conclude that characterized source approach is promising for tsunami prediction.

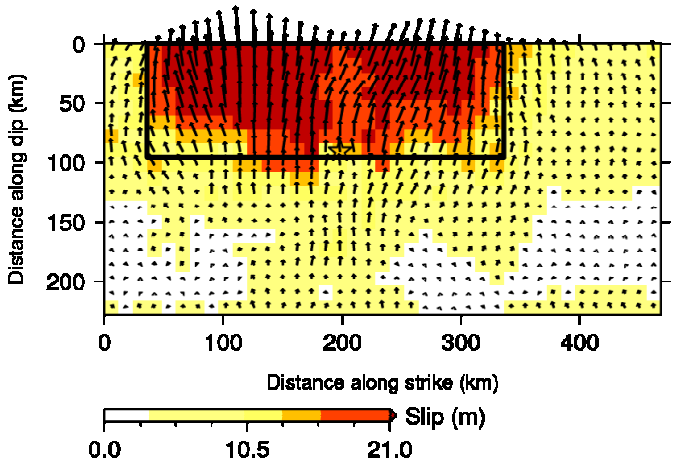

Fig. 7 Result of the source model characterization. Thick line indicates characterized asperity.

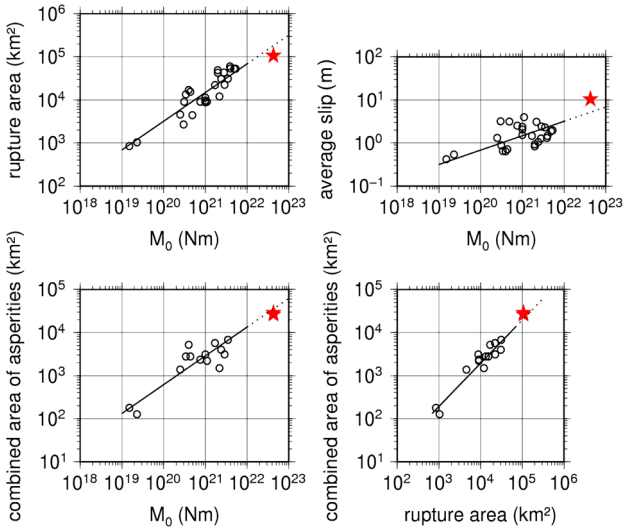

Fig. 8 Comparison of parameters of the characterized source model (star) with average relationships (line) for subduction zone earthquakes (circle)

Table 1 Parameters of the characterized source model

Source parameter	Value
Total rupture area	1.1281×10^{12} m^2
Combined area of asperities	3.1250×10^{10} m^2
Number of asperities	1
Average slip	10.5 m
Asperity slip	22 m
Background slip	6 m

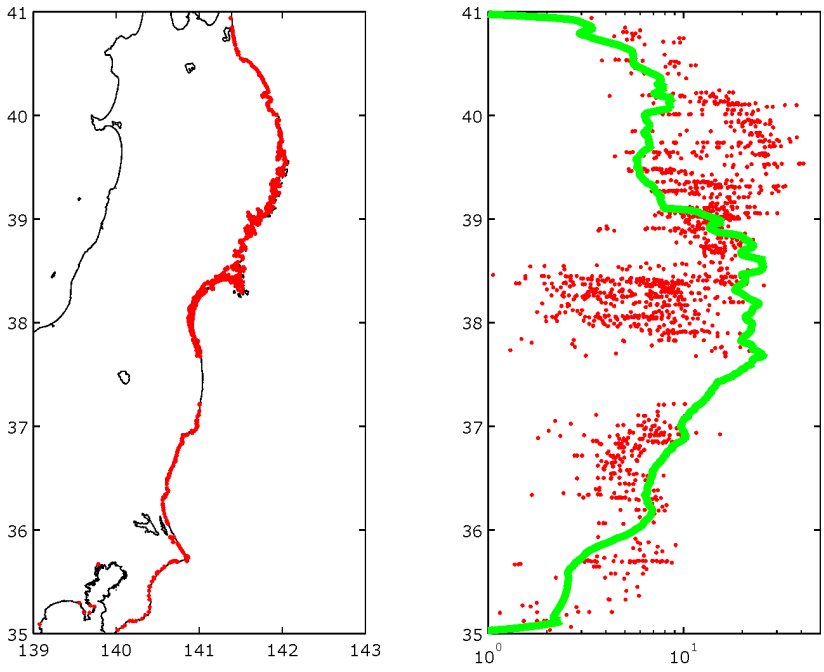

Fig. 9 Right: Comparison of observed inundation heights (dots) and simulated peak values (line) for the characterized source model. Left: Location of observation points

DISCUSSION AND CONCLUSIONS

Tsunami of the 2011 Tohoku earthquake was simulated using source model estimated by inversion of the long-period strong-motion waveform data. Forward tsunami simulation results demonstrate good agreement with observation data, namely tsunami waveforms for off-shore gauges and on-shore inundation heights. We also verified the characterized source model approach, which is widely used for prediction of the strong ground motions. This indicates that source models developed for prediction of strong ground motions can be used for prediction of tsunami too.

In spite of good fit of tsunami waveforms at off-shore gauges, inundation heights on the Sanriku coast are underestimated with a factor of 2. Due to effect of source, first tsunami wave at the off-shore gauge 807 in this area is underestimated with a factor of 1.5. Inundation heights underestimation, corrected for this underestimation due to source, can be reduced to a factor of 1.3. There is a tendency that accurate simulation of the tsunami inundation employing detailed bathymetry data and small finite-difference grid (20-30 m instead of 500 m used in this study) could improve fit with observation data. In another case, an additional tsunami source, north of existing source, maybe necessary to explain high inundation in the North Sanriku Coast. We should notice that existing source is traced by the aftershock distribution and can not be extended to the north. Additional tsunami source may have different nature, submarine landslide for example.

The two-stage tsunami waveforms, having gradual rise and impulsive high amplitude wave were well reproduced with a single plane source model due to localization of tsunami source near the eastern shallow edge of fault plane. This effect of our single plane model may mimic similar effect of the back-stop fault of the real fault model in Japan Trench (Tsuji et al. 2011), or effect of an additional uplift of sediments near a toe of an inner trench slope due to a large horizontal slip (Tanioka and Seno, 2011, Tanioka et al. 2011). 3D curved fault model may be necessary for accurate source modeling and tsunami simulation. For example, inconsistency of simulated narrow peaks with observed wide peaks in the southern part of the model (gauges 801, 803) may be result of this inaccuracy of the fault surface modeling.

ACKNOWLEDGMENTS

We used the tsunami waveform data of the Nationwide Ocean Wave Information network for Ports and Harbours (NOWPHAS), and tsunami field observations of the Joint Tohoku Earthquake Tsunami Survey Group. Bathymetry models are provided by JODC, JAMSTEC and JHA. We are indebt to James Kirby, Philip Watts and Stéphan Grilli, provided tsunami simulation program.

REFERENCES

Bouchon, M. (1981). "A simple method to calculate Green's functions for elastic layered media." *Bull. Seismol. Soc. Am.*, Vol. 71, 959-971.

Hayashi, Y., H. Tsushima, K. Hirata, K. Kimura, and K. Maeda (2011). "Tsunami source area of the 2011 off the Pacific Coast of Tohoku Earthquake determined from tsunami arrival times at offshore observation stations." *Earth Planets Space*, Vol. 63, No. 7, 809-813.

Hayes, G. P. (2011). "Rapid Source Characterization of the 03--11—2011 Mw 9.0 Off the Pacific Coast of Tohoku Earthquake." *Earth Planets Space*, Vol. 63, No. 7, 529-534.

Ide, S., A. Baltay, and G. Beroza (2011). "Shallow dynamic overshoot and energetic deep rupture in the 2011 *M*w 9.0 Tohoku-oki earthquake." *Science*, doi:10.1126/science.1207020.

Ioualalen, M., B. Pelletier, M. Regnier, and P. Watts (2006). "Numerical modeling of the 26th November 1999 Vanuatu tsunami." *J. Geophys. Res.*, Vol. 111, C06030, doi:10.1029/2005JC003249.

Irikura, K., and H. Miyake (2010). "Recipe for Predicting Strong Ground Motion from Crustal Earthquake Scenarios", *Pure Appl. Geophys.*, Vol. 168, No. 1-2, 85-104.

Ito, T., K. Ozawa, T. Watanabe, and T. Sagiya (2011). "Slip distribution of the 2011 Tohoku earthquake inferred from geodetic data." *Earth Planets Space*, Vol. 63, No. 7, 627-630.

Kennet, B. L. N, and N. J. Kerry (1979). "Seismic waves in a stratified half space." *Geophys. J. R. Astr. Soc.*, Vol. 57, 557-583, 1979.

Kurahashi, S. and K. Irikura (2011). "Source model for generating strong ground motions during the 11 March 2011 off the Pacific Coast of Tohoku Earthquake." *Earth Planets Space*, Vol. 63, No. 7, 571-576.

Lay, T., C. J. Ammon, H. Kanamori, Lian Xue1, and M. J. Kim (2011). "Possible large near-trench slip during the great 2011 Tohoku (*M*w 9.0) Earthquake", *Earth Planets Space*, Vol. 63, No. 7, 687-692.

Murotani, S., H. Miyake, and K. Koketsu (2008). "Scaling of characterized slip models for plate-boundary earthquakes" *Earth Planets Space*, Vol. 60, 987–991.

Okada, S. (1985). "Surface displacement due to shear and tensile faults in a half-space." *Bull. Seismol. Soc. Am.*, Vol. 75, 1135–1154.

Satake, K., S. Sakai, Y. Fujii, M. Shinohara, and T. Kanazawa (2011). "Tsunami Source of 2011 Tohoku Earthquake." *Kagaku*, Vol. 81, 407-410.

Somerville, P., K. Irikura, R. Graves, S. Sawada, D. Wald, N. Abrahamson, Y. Iwasaki, T. Kagawa, N. Smith, and A. Kowada (1999). "Characterizing earthquake slip models for the prediction of strong ground motion". *Seismol. Res. Lett.*, Vol. 70, 59–80.

Tanioka, Yu., and T. Seno (2001). "Sediment effect on tsunami generation of the 1896 Sanriku tsunami earthquake." *Geophys. Res Lett.*, Vol. 28, No. 17, 3389-3392.

Tanioka, Y., A.R. Gusman, H. Tsushima, and S. Sakai (2011). "Source process of the 2011 Tohoku earthquake estimated from the joint inversion of tsunami waveforms, onshore GPS, and seafloor deformation data." *The Seismological Sociaty of Japan, 2011 Fall Meeting, Programme and Abstracts*, A11-02, p.3.

Tsuji, T., Yo. Ito, M. Kido, Yu. Osada, H. Fujimoto, J. Ashi, M. Kinoshita, and T. Matsuoka (2011). "Potential tsunamigenic faults of the 2011 off the Pacific coast of Tohoku Earthquake." *Earth Planets Space*, Vol. 63, No. 7, 831–834.

Watts, P., Grilli, S. T., Kirby, J. T., Fryer, G. J., and Tappin, D. R. (2003). “Landslide tsunami case studies using a Boussinesq model and a fully nonlinear tsunami generation model.” *Nat. Hazards and Earth Sci. Systems, EGU*, Vol. 3, No. 5, 391-402.

Wei, G., and J. T. Kirby (1995). “A time-dependent numerical code for extended Boussinesq equations.” *J. Waterw. Port Coastal Oceanic Eng.,* Vol. 121, 251– 261.

Yoshida, K., K. Miyakoshi, and K. Irikura (2011). “Source Process of the 2011 Off the Pacific Coast of Tohoku Earthquake Inferred from Waveform Inversion with Long-Period Strong-Motion Records.” *Earth Planets Space*, Vol. 63, No. 7, 577-582.